Published in final edited form as:
Exp Cell Res. 2010 March 10; 316(5): 813–825. doi:10.1016/j.yexcr.2010.01.013.

Mesenchymal cells stimulate capillary morphogenesis via distinct proteolytic mechanisms

Cyrus M Ghajar[a], **Suraj Kachgal**[a], **Ekaterina Kniazeva**[a], **Hidetoshi Mori**[b], **Sylvain V Costes**[b], **Steven C George**[a,c,*,#], and **Andrew J Putnam**[a,c,d,**,#]

[a]Department of Biomedical Engineering, University of California, Irvine, Irvine, CA 92697

[b]Department of Cancer & DNA Damage Responses, Life Sciences Division, Lawrence Berkeley National Laboratory, Berkeley, CA 94720

[c]Department of Chemical Engineering and Materials Science, University of California, Irvine, Irvine, CA 92697

[d]Department of Biomedical Engineering, University of Michigan, Ann Arbor, MI, 48109

Abstract

During angiogenesis, endothelial cells (ECs) degrade their surrounding extracellular matrix (ECM) to facilitate invasion. How interactions between ECs and other cells within their microenvironment facilitate this process is only partially understood. We have utilized a tractable 3D co-culture model to investigate the proteolytic mechanisms by which pre-committed or more highly committed mesenchymal cells stimulate capillary formation. On their own, ECs invade their surrounding matrix, but do not form capillaries. However, in the presence of either mesenchymal stem cells (MSCs) or fibroblasts, ECs form polarized, tubular structures that are intimately associated with mesenchymal cells. Further, ECs upregulate gene expression of several extracellular proteases upon co-culture with either mesenchymal cell type. The administration of both broad spectrum and specific protease inhibitors demonstrated that MSC-stimulated capillary formation relied solely on membrane-type matrix metalloproteinases (MT-MMPs) while fibroblast-mediated sprouting proceeded independent of MMP inhibition unless the plasminogen activator/plasmin axis was inhibited in concert. While other studies have established a role for the ECM itself in dictating proteolysis and matrix degradation during capillary morphogenesis, the present study illustrates that heterotypic cellular interactions within the microenvironment can direct the proteolytic mechanisms required for capillary formation.

Keywords

Capillary Morphogenesis; Angiogenesis; Fibroblasts; Mesenchymal Stem Cells; Matrix Metalloproteinases; Microenvironment

*__Correspondence:__ Department of Biomedical Engineering, Engineering Hall, Room 2420, University of California, Irvine, Irvine, CA 92697-2730. scgeorge@uci.edu, Telephone: 949.824.3941, Fax: 949.824.9968. **Department of Biomedical Engineering, 2154 LBME Building, University of Michigan, Ann Arbor, MI 48109-2110. putnam@umich.edu, Telephone: 734.615.1398.
[#]authors contributed equally to this manuscript

Introduction

Angiogenesis, the sprouting of new vasculature from a pre-existing vascular network, is a process crucial to the growth and maintenance of tissues 1. Understanding the mechanisms that govern this complex process may facilitate approaches to engineer tissues for regenerative medicine purposes [2] and treat pathologies (e.g., cancer and diabetic retinopathy) characterized by misregulated vessel formation and maintenance [3].

A cell's microenvironment, composed of its surrounding extracellular matrix (ECM), other cells, and factors (e.g., soluble proteins) secreted as a result of interactions between these constituents[4], profoundly influences cell behavior 5, 6. In the context of capillary morphogenesis, the identity 7 and concentration 8–13 of ECM molecules regulate endothelial cell (EC) invasion and tube formation. Homotypic (EC-EC) interactions are crucial to guiding and sustaining this morphogenic process 14, 15, while heterotypic interactions with other cell types (e.g., tumor cells or interstitial cells) also promote capillary morphogenesis through the production of numerous angiogenic factors 16. Extracellular proteases, especially those comprising the matrix metalloproteinase (MMP) and serine protease families 17, 18, are amongst these factors, as they facilitate ECM degradation (in addition to several other functions, reviewed in 19), which is necessary for EC invasion to occur.

Macromolecules within the ECM dictate the proteases utilized by ECs for the purposes of invasion. For instance, capillary invasion in type I collagen matrices depends critically on membrane-bound MMP14 (also known as MT1-MMP) [20], while invasion of the provisional clot (composed primarily of the plasma protein fibrinogen in its cleaved form, fibrin)present in wounds, sites of inflammation, and tumors may depend less on MMPs and more on the serine proteases that comprise the plasminogen activator (PA)/plasmin axis 21, 22. However, in more complex tissue explant cultures, capillary invasion in fibrin matrices proceeds independent of the PA/plasmin axis and relies instead on MT-MMP activity 23. These results imply that in addition to the ECM, other cell types have the potential to bias the proteases utilized by ECs to undergo capillary morphogenesis.

The present study explores whether different stromal cell types modulate EC proteolysis via distinct mechanisms during capillary morphogenesis in a three-dimensional (3D) ECM. Using an established co-culture model [9, 10, 24] that generates true capillaries that are functional *in vivo* [25], we show that two mesenchymal cell types (mesenchymal stem cells (MSCs) and fibroblasts) guide ECs to undergo a virtually complete angiogenic program via distinct proteolytic mechanisms. Specifically, ECs rely solely on MT-MMPs to undergo capillary morphogenesis in EC-MSC co-cultures, but utilize MMPs and the PA/plasmin axis to form capillary networks when co-cultured with fibroblasts. These data demonstrate that in addition to the ECM, interactions with other cell types determine the proteolytic repertoire utilized by ECs to undergo capillary morphogenesis, and point further to the importance of the integrated microenvironment in regulating cell behavior.

Materials and Methods

Construction of a 3D co-culture model to study capillary morphogenesis and quantify vessel networks

Construction of the 3D co-culture model was performed as described previously 10. In brief, mCherry-transduced human umbilical vein ECs (p3-p4) were cultured on Cytodex™ microcarrier beads (Sigma-Aldrich Co., St. Louis, MO) and mixed with either normal human lung fibroblasts (Lonza Biologics Inc., Portsmouth, NH; used prior to p10) or MSCs (Lonza, used at p4 or p5) within a 2.5 mg/mL fibrin matrix (the approximate physiologic clotting concentration of fibrin 26). Medium (EGM-2, Lonza) was added after clotting and changed at

days 1, 3, and 5. For studies involving inhibitors, the appropriate vehicle or inhibitor(s) was mixed withmedium prior to addition to the culture. For non-small molecule inhibitors (e.g., antibodies), the inhibitor was added at the indicated concentration in the fibrinogen solution prior to clotting and to the culture medium as well. Inhibitors were added at the following concentrations: GM6001, 10–40 μM (Calbiochem, San Diego, CA); BB2516, 3.3–10 μM (Tocris Bioscience, Ellisville, MO); aprotinin, 2.2 μM (Sigma); ε-aminocaproic acid, 50 mM (Sigma); human tissue inhibitor of metalloproteinase (TIMP)1, 5 μg/mL (R&D Systems, Minneapolis, MN); human TIMP2, 5 μg/mL (R&D Systems); a function-blocking antibody directed towards the urokinase plasminogen activator receptor (uPAR), 25 μg/mL (American Diagnostica, Inc., Stamford, CT); a function-blocking antibody targeting HGF, 1 μg/mL and 10 μg/mL (R&D Systems) 27; and a neutralizing antibody directed at TNFα, 1 μg/mL and 10 μg/mL (Abcam, Cambridge, MA).

Low magnification (4x, to image as large a field as possible) fluorescent images of isolated beads were randomly captured at day 7. To maximize objectivity, an automated approach was adapted to quantify the total length of the vascular networks. Images were processed in a batch mode, using a script based on the *Angiogenesis Tube Formation Application Module* in Metamorph imaging software (Molecular Devices, Sunnyvale, CA). Briefly, each image was segmented based on a constant threshold of a background corrected image. The *Adaptive Background Correction*™ function of Metamorph was used to crrect uneven image backgrounds throughout the image by adapting to local content. This allowed for more robust segmentation and analysis Any tubule-like pattern of the image less than a specified minimum width was considered to be noise and was excluded from the segmentation. A maximum width was used to differentiate tubules from beads. A sample image of network tracings, visualized and reconstructed in Imaris (Bitplane AG, Zurich, Switzerland), is presented in Figure 1.

For association studies, fibroblasts or MSCs were first retrovirally transduced with a green fluorescent protein (GFP) retrovirus as described previously [10]. Tissue construction and maintenance then proceeded exactly as described. Imaging was conducted on day 7.

Immunofluorescent Staining

Cultures were constructed within 8 well LabTek™ chamberslides with a No.1 thickness borosilicate bottom (ThermoFisher Scientific; Rochester, NY) and maintained until the appropriate timepoint. Samples were fixed in formalin for 10 minutes, permeabilized for 10 min, and blocked in a 2% solution of bovine serum albumin in TBS-T for 1 hour. Primary antibody/staining agent was diluted in blocking solution at the appropriate concentration (collagen IV, 1:200 (Sigma); phalloidin, 1:50 (Molecular Probes, Eugene, OR); alpha-smooth muscle actin (αSMA), 1:200 (Sigma); NG2, 1:200 (Chemicon International, Inc., Temecula, CA)) and incubated with the gel at 4°C for 2.5 hours. Samples were washed in TBS-T overnight and incubated with the appropriate secondary antibody (1:200) the next day (2 hours at 4°C). After another overnight wash, samples were incubated with a 250 μM solution of DAPI (in PBS) for 10 minutes in order to visualize nuclei, washed, and finally imaged on a Zeiss LSM 510 Meta multiphoton confocal microscope (Carl Zeiss, Inc.; Jena, Germany). Images obtained were 12 bit images containing 1024× 1024 pixels. Four scans were averaged per pixel.

DQ Collagen Cultures

To visualize the localization of proteolytic activity in EC/mesenchymal cell co-cultures, 1% (v/v) of a 2.5 mg/ml solution of DQ collagen, type I (Molecular Probes) was added to the 2.5 mg/ml fibrinogen solution prior to polymerization. Gels were constructed as described above within 8 well No. 1 thickness Labtek chamberslides and imaged at day 7 using the Zeiss LSM 510 Meta. Image slices were acquired every 5 microns and reconstructed using Zeiss LSM Image Browser.

RNA Isolation

For each condition and timepoint, 24 tissues containing >100 HUVEC-coated beads +/− 25K overlying fibroblasts or MSCs each was constructed. To isolate RNA from fibroblast or MSC monolayers, gels were twice washed with PBS, then 100 μl of a concentrated trypsin solution (2.5%; Sigma) was added until the monolayer was completely removed (30–60 seconds). Trypsin was immediately neutralized with 200 μl of Media 199 (Invitrogen; Carlsbad, CA) containing 20% fetal bovine serum (FBS). Neutralized solutions were collected, spun down for 5 minutes at 200*g*, lysed using RNA lysis buffer (Qiagen; Valencia, CA), and stored at −80 °C.

To isolate EC, gels stripped of mesenchymal cell monolayers or gels containing only EC-coated microcarriers were washed with PBS before dislodging gels from the well siding using a small spatula. Gels were subsequently dissolved by adding 500 μl of trypsin (2.5%) and incubating at 37°C for ~20 minutes with periodic agitation. Upon dissolution, 1 ml of M199 containing 20% FBS and 1% P/S was added to quench trypsin activity. To ensure complete removal of EC from microcarriers, the contents of each well were triturated via repeated pipetting. The contents of each well were collected, microcarrier beads were removed by gravity, and the remaining solution was centrifuged to collect ECs. ECs were suspended in RNA lysis buffer before storage at −80°C.

Determination of mRNA transcript levels via RT-PCR

RT-PCR was conducted to analyze the expression of several genes in fibroblasts, MSCs, or ECs. Table I lists the genes analyzed.

Total RNA was isolated from samples using the RNeasy kit (Qiagen) per manufacturer's protocol. The concentration of purified RNA was quantified using the Quant-iT™ RiboGreen RNA assay kit (Molecular Probes) according to the manufacturer's instructions. Equal amounts of total RNA from each sample were used to synthesize cDNA templates using the AMV reverse transcriptase kit (Promega; Madison, WI), also according to manufacturer's protocol. The cDNA for each sample (2 μl) was amplified via PCR for 35 cycles in a total reaction volume of 50 μl. The reaction mixture was comprised of 200 nM of the appropriate forward and reverse primers, 0.2 mM deoxynucleoside triphosphate, 1.5 mM $MgCl_2$, and 1U of Taq polymerase (Promega). For each gene analyzed, forward and reverse primer sequences, annealing temperature, and amplicon size are listed in Table I. Amplified products were resolved via electrophoresis through 2% agarose gels containing 0.05% ethidium bromide, visualized using a BioRad ChemiDoc XRS imaging system (BioRad Laboratories; Hercules, CA), and verified via comparison of the known amplicon size with a DNA ladder. Images were inverted to facilitate visualization of bands.

Statistical Analyses

Data are presented as mean ± S.D. Statistical analyses were conducted using SigmaStat 3.5 (Systat Software, Inc., San Jose, CA), with p values < 0.05 deemed significant. The specific method of statistical analysis used for a given experiment is described in the appropriate figure legend.

Results

MSCs and fibroblasts stimulate ECs to form mature capillary networks

Capillary sprouting can be divided into four distinct steps, including: EC invasion and proliferation, primitive tube formation, stabilization of nascent tubules (which involves basement membrane deposition and pericytic association) and pruning of the vascular network [1]. EC sprouting in MSC- or fibroblast-laden ECMs was monitored over a 7 day period to

determine whether both mesenchymal cell types stimulate ECs to undergo these steps. ECs were transduced to express the red fluorescent protein mCherry in order to differentiate capillary networks form surrounding interstitial cells.

ECs invaded surrounding ECM as early as day 1, formed primitive tubular structures by day 3, and elaborated into extensive vascular networks by day 7 (Fig. 2A and A'). In both culture conditions (EC-MSC and EC-fibroblast), vessels were surrounded by basement membrane sleeves, as gauged by IF staining cultures for collagen IV, which is a prominent component of the vascular basement membrane [7] (Fig. 2B and B', see white arrows). Vascular mural cells, or pericytes stabilize nascent endothelium and are characterized by physical association with ECs as well as expression of molecular markers such as αSMA and NG2 [28]. MSCs and fibroblasts both exhibited pericytic behavior: these mesenchymal cell types intimately associated with capillaries, demonstrated by co-culture of GFP-MSCs or GFP-fibroblasts with mCherry-ECs (Fig. 2C and C'). IF staining revealed that MSCs ubiquitously expressed αSMA in addition to occasional NG2 expression (Fig. 2D), while EC-associated fibroblasts only stained positively for αSMA (Fig. 2D'). Collectively, these results demonstrate that both uncommitted MSCs and their differentiated progeny guide ECs to form mature vascular networks in 3D co-cultures.

Mesenchymal cell-mediated capillary morphogenesis is accompanied by enhanced periendothelial proteolysis

Localized proteolytic activity is necessary to facilitate key steps of the angiogenic cascade [23, 29–31]. We have previously observed that the addition of mesenchymal cells contributes to bulk increases of MMP levels in 3D cultures [9]. However, whether the mesenchymal cells were directly responsible for the enhanced proteolytic activity observed or whether these cells were inducing increased proteolytic activity by ECs was unclear. To visualize localized proteolytic activity, 3D ECMs were doped with a small amount (1%) of a fluorescein-laden substratum (DQ Collagen, type I), which emits a green fluorescent signal upon cleavage by collagenases.

As shown previously [24], ECs cultured in the absence of interstitial cells (or even in the presence of medium conditioned by interstitial cells [24, 32]) do not form capillary-like structures under these conditions, but do invade the surrounding fibrin ECM. ECs cultured alone elicited a focal signal from the DQ substratum (Fig. 3A). Conversely, a strong, primarily periendothelial DQ signal was observed in both EC-MSC (Fig. 3B) and EC-fibroblast (Fig. 3C) co-cultures.

To confirm this apparent upregulation in periendothelial proteolysis, rather than spread mesenchymal cells throughout EC-containing matrices, MSCs or fibroblasts were seeded on top of fibrin matrices. This co-culture method allowed the effective isolation of ECs from mesenchymal cells in order to determine how cross-talk between these spatially distinct cell populations affected transcript expression of each cell type [24]. MSCs and fibroblasts both stimulated robust capillary network formation by 7 days with this altered configuration. Again, ECs cultured within the 3D ECM on their own invaded the surrounding ECM but did not form capillary-like structures (Fig. 4A). We examined mRNA expression levels of both mesenchymal and endothelial cell populations at day 1, day 3, and day 7 via RT-PCR. The mRNA expression of several fibrinolytic enzymes-- including MT1-, MT2-, and MT3-MMP, MMP2 and MMP9, and members of the PA/plasmin axis including tissue PA (tPA), urokinase-type PA (uPA), and uPAR-- was probed. The most notable differences in expression were observed at day 3 (Fig. 4B), which coincided with the time point that ECs were first observed to form lumen-containing structures in co-cultures (Fig. 4A, middle column, white arrows).

Aside from MT1-MMP expression, which was increased by fibroblasts upon culture with ECs, neither mesenchymal cell type altered its expression of the fibrinolytic enzymes investigated

in response to culture with ECs (Fig. 4B). However, it was apparent that fibroblasts expressed much higher levels of uPA transcript than MSCs (Fig. 4B). This result was confirmed at the protein level both by Western blot and plasminogen zymography (data not shown). On the other hand, ECs only expressed MT3-MMP, uPAR, and tPA when cultured alone. However, upon culture with MSCs, EC expression of MT1-MMP, MT3-MMP, MMP2, and MMP9 was strongly increased (Fig. 4B). In contrast, ECs exhibited a drastic increase in MT3-MMP expression along with decreased uPAR expression when cultured with fibroblasts (Fig. 4B). Taken together, the data presented in Figure 3 and Figure 4 suggest that: 1) MSCs and fibroblasts induce increased proteolytic activity in the periendothelial compartment, 2) MSCs and fibroblasts each upregulate EC expression of fibrinolytic enzymes in signature fashion, and 3) that this enhancement early on is crucial to the morphogenic process. We thus applied broad spectrum protease inhibitors to determine whether MSC- and fibroblast-mediated sprouting proceed through different proteolytic mechanisms.

Broad spectrum protease inhibition suggests that MSCs and fibroblasts stimulate capillary morphogenesis through different proteolytic mechanisms

To test the proteolytic dependence of MSC- and fibroblast-mediated capillary morphogenesis, co-cultures were treated with increasing concentrations of the broad spectrum MMP inhibitor GM6001 [33], the serine protease inhibitor aprotinin, or a combination of the two ("dual," Fig. 5–Fig. 6).

MSC-mediated sprouting was drastically inhibited by the application of broad-spectrum MMP inhibitors when compared to vehicle (DMSO)-treated conditions (Fig. 5). Doses of GM6001 (10, 20, 40 μM) nearly 1000x greater than IC_{50} values reported for several MMPs (e.g., MMP2, MMP9, MT1-MMP 34) abrogated network formation at every concentration tested (Fig. 5A–B). To lessen the probability of off-target effects, a second broad spectrum MMP inhibitor was applied to these cultures. BB2516, which has IC_{50} values that are roughly one third of those measured for GM6001 (as reported by the manufacturer), also virtually eliminated capillary formation at both concentrations tested (3.3 and 10 μM) (Fig. 5B). On the other hand, application of an endogenous serine protease inhibitor (aprotinin, 2.2 μM 35) had no effect on the formation of vascular networks, demonstrating that capillary network formation proceeds independent of plasmin-mediated proteolysis in EC-MSC cultures (Fig. 5A–B). As expected, inhibiting MMPs and serine proteases in concert eliminated network formation (Fig. 5A–B).

A strikingly different response to protease inhibition was noted in EC-fibroblast cultures (Fig. 6). GM6001 did not affect fibroblast-stimulated capillary network formation when compared to vehicle-treated conditions; only a 40 μM dose of the inhibitor significantly reduced, but did not eliminate, sprouting (Fig. 6A–B). Similar results were obtained with BB2516 (Fig. 6B). The serine protease inhibitor aprotinin also did not alter network formation. However, dual application of GM6001 (10 μM) and aprotinin (2.2 μM) eliminated network formation (Fig. 6A–B). The synergistic nature of combinatorial MMP and serine protease inhibition was confirmed using BB2516 in place of GM6001 and/or by replacing aprotinin with ε-aminocaproic acid (EACA, 50mM), which inhibits the association of plasmin and fibrin [36] (data not shown).

In sum, these data demonstrate that MSC- and fibroblast-mediated capillary morphogenesis proceed via distinct proteolytic mechanisms and suggest specifically that MSC-mediated sprouting is driven solely by MMPs. More specific endogenous MMP inhibitors were applied to confirm this result.

Specific inhibition reveals that MSC-stimulated capillary morphogenesis depends on MT-MMP activity

To eliminate the potential off-target effects associated with synthetic small molecule inhibitors such as GM6001 and BB2516, endogenous MMP inhibitors were applied to EC-MSC and EC-fibroblast co-cultures. Compared to a vehicle control, TIMP1, which inhibits soluble MMP activity [37], did not affect MSC- (Fig. 7A, B) or fibroblast-mediated network formation (Fig. 7A, C). Conversely, TIMP2, which inhibits the activity of membrane-bound and soluble MMPs [37], severely compromised sprouting in EC-MSC co-cultures (Fig. 7A–B) but had no effect on network formation in EC-fibroblast co-cultures (Fig. 7A, C), suggesting that MT-MMPs play a critical role in MSC-mediated sprouting. A function blocking antibody targeting uPAR did not restrict network formation in either case, confirming that the activity of this key membrane-bound member of the PA/plasmin axis is not crucial for MSC- or fibroblast-mediated sprouting on its own.

Discussion

It is now well-established that MMPs and the PA/plasmin axis play important roles in EC invasion during capillary morphogenesis. How other cell types influence the proteolytic means by which ECs conduct this process is less clear. In the present work, we have utilized a co-culture model which recapitulates most phases of angiogenesis, including EC invasion, nascent tube formation, and stabilization of these tubes by both pericytic association and basement membrane deposition [1], to demonstrate that both multi-potent MSCs and more committed fibroblasts stimulate capillary morphogenesis within 3D fibrin ECMs, but do so via distinct proteolytic mechanisms. Specifically, MSC-mediated capillary formation relied solely on MMPs, while fibroblast-mediated capillary formation proceeded in spite of MMP inhibition unless the PA/plasmin axis was inhibited in concert. Collectively, these data demonstrate that the cellular component of the microenvironment influences the proteolytic means by which ECs undergo capillary morphogenesis.

Mesenchymal cells stimulate an increase in the transcript expression of extracellular proteases by ECs early on, and this appears to be key to stimulating the morphogenic program. In the presence of several angiogenic factors present in the culture medium, ECs invaded the surrounding fibrin ECM but failed to form vessels when cultured on their own. Co-culture with mesenchymal cells stimulated the formation of capillary-like structures as early as day 3, and RT-PCR revealed that tube formation coincided with an induction of fibrinolytic enzymes at this time point. However, differences in the pattern of transcript upregulation induced by MSCs and fibroblasts were evident, and may underlie the functional differences observed when inhibitor studies were performed with both exogenous and endogenous protease inhibitors. For instance, co-culture with MSCs resulted in enhanced EC expression of MT1-MMP, MT3-MMP, MMP2, MMP9, and uPAR. This expression pattern suggested that MSC-mediated sprouting relies on MMP induction, and indeed sprouting in EC-MSC cultures was ablated by the broad spectrum MMP inhibitors GM6001 and BB2516. TIMP-based studies further specified that MSC-mediated sprouting depends on MT-MMPs.

In contrast, co-culture with fibroblasts only stimulated enhanced expression of MT3-MMP by ECs. But when compared to MSCs, fibroblasts expressed significantly higher levels of uPA at both the transcript and protein levels. Interestingly, functional assays revealed that sprouting persisted in EC-fibroblast cultures in spite of MMP inhibition. Furthermore, serine protease inhibition (via aprotinin) did not alter vascular network formation, either. Instead, dual application of MMP and serine protease/plasmin inhibitors was necessary to block capillary network formation. Thus, in fibrin gels, fibroblasts appear to stimulate ECs to expand their proteolytic repertoire and utilize both the MMP and PA/plasmin axes while undergoing capillary morphogenesis.

The mechanisms underlying this behavior are unclear. While plasmin activates a number of MMPs [37], it is unlikely that an increase in the bulk concentration of plasmin (due to the increased levels of uPA activity observed in fibroblast cultures) results in levels of MMP activity that overwhelm either MMP inhibitor used, as each was applied at a dose that exceeded its reported IC_{50} values by greater than 1000-fold. Instead, it is plausible that in fibroblast-EC cultures, a third type extracellular protease (e.g., cysteine cathepsins 18) is involved in the morphogenic process, and its activity is not quenched until both MMP and plasmin activity is inhibited.

Disparate growth factor secretion profiles may also underlie the differences observed in the proteolytic mechanisms utilized by ECs as they sprout in EC-MSC vs. EC-fibroblast cultures. We did not exhaustively explore this possibility, but did examine some likely candidates: VEGF, which signals through VEGF receptors to increase MT1-MMP expression [38]; HGF, shown to induce MT1-MMP, MMP2, uPA, and uPAR expression in cancer cells [39, 40]; and TNFα, which enhances uPAR expression by ECs [41]. As shown in Supplemental Figure 1, sprouting in both EC-MSC and EC-fibroblast cultures was partially mediated by exogenous VEGF and endogenous HGF, but proceeded fully despite TNFαinhibition. Notably, differences were not observed between the two culture conditions.

We also considered that fibroblasts may directly or indirectly alter the deposition and arrangement of proteins in the periendothelial compartment [42], in turn affecting the dynamics of uPAR on the EC surface. We were unable to determine surface localization of uPAR in 3D culture using a fluorescently conjugated antibody targeting the membrane-bound receptor [42], and sprouting persisted in these cultures despite the addition of a function blocking antibody that specifically targets uPAR. Ablation of surface bound uPAR will be necessary to conclusively determine if this membrane-bound member of the PA/plasmin axis is a key node in the MMP-independent form of capillary morphogenesis observed in EC-fibroblast cultures.

A number of prior studies have demonstrated that another principle component of the microenvironment, the ECM, alters the proteolytic landscape utilized to facilitate morphogenic events. This is the case not only for capillary morphogenesis, but branching morphogenesis of mammary and salivary epithelia [43, 44]. Of course, substrate specificity comes into play, as some proteases are restricted to digesting a handful of ECM molecules, while others are less selective [37]. Though several MMPs are capable of cleaving type I collagen [37], MT1-MMP is indispensable for invasion and capillary lumen formation within collagen I matrices [20, 45, 46]. In fibrin, the story is not as straightforward. Homotypic culture models have demonstrated that EC invasion of fibrin matrices relies solely on uPAR and not on MMPs 21, 22, 47. However, other models have demonstrated EC tubulogenesis within fibrin matrices is MT-MMP dependent (though not necessarily dependent on MT1-MMP) when ECs are stimulated by either a broad array of growth factors 48 or by other cell types (such as in a mouse aortic vessel explant assay 20). Indeed, endowing MT-MMP naïve cells with either MT1-, MT2- or MT3-MMP is sufficient to confer them with the ability to invade fibrin 49. Thus, the ability of MT1-null aortic explants to sprout in fibrin 20 may be the result of heterotypic interactions which tune the cell surface proteases utilized by ECs as they undergo this morphogenic program. The data presented here suggest that changing the identity of the cell type on the other end of this heterotypic interaction can also modulate the proteases utilized by ECs to facilitate capillary morphogenesis.

A final implication of the present work is that the systems used in this study can be applied to model physiological and pathological angiogenesis. Recent work demonstrated that MSCs occupy a perivascular niche in a variety of organs and function as pericytes with multi-lineage potential [50]. Coupled with their ability to home to sites of injury [51] and foster a regenerative microenvironment via trophic activities [52, 53], it is tempting to speculate that both bone marrow-

derived and resident tissue MSCs function physiologically to aid in the repair of damaged mesenchyme, in part by stimulating and stabilizing neovasculature. We noticed a qualitative reduction in vessel coverage by fibroblasts compared to MSCs (Figs. 2C and C'). Pericytic investment stabilizes vessels and protects EC from apoptosis [54], and reduced or sporadic vessel coverage is a hallmark of the reactive stroma present in chronic wounding disorders and surrounding carcinomas 55, as is sustained fibroblast activation to the myofibroblast phenotype 56, 57 (marked by αSMA expression, which was observed in this and our prior study 10). Thus, the EC-MSC model of capillary morphogenesis may effectively simulate physiologic conditions while the EC-fibroblast model simulates pathological neovascularization. If true, this demonstrates the importance of using appropriate experimental models to uncover effective therapies for a given process. For instance, the failures of broad spectrum MMP inhibitors to effectively halt tumor dissemination and pathologic angiogenesis are well documented 58. The present study illustrates how modeling complex interactions in appropriate experimental models could uncover novel approaches to address these shortcomings.

Supplementary Material

Refer to Web version on PubMed Central for supplementary material.

Abbreviations

3D	three-dimensional
αSMA	alpha-smooth muscle actin
EACA	ε-aminocaproic acid
EC	endothelial cell
ECM	extracellular matrix
GFP	green fluorescent protein
IF	immunofluorescent
MMP	matrix metalloproteinase
MSC	mesenchymal stem cell
MT-MMP	membrane-type matrix metalloproteinase
PA	plasminogen activator
TIMP	tissue inhibitor of metalloproteinases
uPA	urokinase-type plasminogen activator
uPAR	urokinase plasminogen activator receptor
tPA	tissue plasminogen activator

Acknowledgments

We thank Dr. Mina J. Bissell for contributing resources. We are grateful to Dr. Martin Nakatsu and to Joseph Harris for aiding in RNA isolation and the design of primers used for RT-PCR, respectively. We are also grateful to Dr. Christopher Hughes, Dr. Chirag Khatiwala, Dr. Valeria Caiolfa, Dr. Nicolai Sidenius, and Dr. Christopher Raub for helpful discussions. This work was supported by grants from the NIH (R01HL085339 to AJP and R01HL067954 to SCG) and the NSF (CBET-0644968 to AJP). CMG was partially supported by a joint scholarship from the ARCS Foundation and Arnold and Mabel Beckman Foundation.

References

1. Jain RK. Molecular regulation of vessel maturation. Nat Med 2003;9:685–693. [PubMed: 12778167]
2. Griffith LG, Naughton G. Tissue engineering--current challenges and expanding opportunities. Science 2002;295:1009–1014. [PubMed: 11834815]
3. Folkman J. Angiogenesis in cancer, vascular, rheumatoid and other disease. Nat Med 1995;1:27–31. [PubMed: 7584949]
4. Bissell MJ, Labarge MA. Context, tissue plasticity, and cancer: are tumor stem cells also regulated by the microenvironment? Cancer Cell 2005;7:17–23. [PubMed: 15652746]
5. Dolberg DS, Bissell MJ. Inability of Rous sarcoma virus to cause sarcomas in the avian embryo. Nature 1984;309:552–556. [PubMed: 6203040]
6. Illmensee K, Mintz B. Totipotency and normal differentiation of single teratocarcinoma cells cloned by injection into blastocysts. Proc Natl Acad Sci U S A 1976;73:549–553. [PubMed: 1061157]
7. Davis GE, Senger DR. Endothelial extracellular matrix: biosynthesis, remodeling, and functions during vascular morphogenesis and neovessel stabilization. Circ Res 2005;97:1093–1107. [PubMed: 16306453]
8. Deroanne CF, Lapiere CM, Nusgens BV. In vitro tubulogenesis of endothelial cells by relaxation of the coupling extracellular matrix-cytoskeleton. Cardiovasc Res 2001;49:647–658. [PubMed: 11166278]
9. Ghajar CM, Blevins KS, Hughes CC, George SC, Putnam AJ. Mesenchymal stem cells enhance angiogenesis in mechanically viable prevascularized tissues via early matrix metalloproteinase upregulation. Tissue Eng 2006;12:2875–2888. [PubMed: 17518656]
10. Ghajar CM, Chen X, Harris JW, Suresh V, Hughes CC, Jeon NL, Putnam AJ, George SC. The effect of matrix density on the regulation of 3-D capillary morphogenesis. Biophys J 2008;94:1930–1941. [PubMed: 17993494]
11. Ingber DE, Folkman J. How does extracellular matrix control capillary morphogenesis? Cell 1989;58:803–805. [PubMed: 2673531]
12. Mammoto A, Connor KM, Mammoto T, Yung CW, Huh D, Aderman CM, Mostoslavsky G, Smith LE, Ingber DE. A mechanosensitive transcriptional mechanism that controls angiogenesis. Nature 2009;457:1103–1108. [PubMed: 19242469]
13. Vailhe B, Lecomte M, Wiernsperger N, Tranqui L. The formation of tubular structures by endothelial cells is under the control of fibrinolysis and mechanical factors. Angiogenesis 1998;2:331–344. [PubMed: 14517453]
14. Lee S, Chen TT, Barber CL, Jordan MC, Murdock J, Desai S, Ferrara N, Nagy A, Roos KP, Iruela-Arispe ML. Autocrine VEGF signaling is required for vascular homeostasis. Cell 2007;130:691–703. [PubMed: 17719546]
15. Korff T, Augustin HG. Tensional forces in fibrillar extracellular matrices control directional capillary sprouting. J Cell Sci 1999;112(Pt 19):3249–3258. [PubMed: 10504330]
16. Yancopoulos GD, Davis S, Gale NW, Rudge JS, Wiegand SJ, Holash J. Vascular-specific growth factors and blood vessel formation. Nature 2000;407:242–248. [PubMed: 11001067]
17. Ghajar CM, George SC, Putnam AJ. Matrix metalloproteinase control of capillary morphogenesis. Crit Rev Eukaryot Gene Expr 2008;18:251–278. [PubMed: 18540825]
18. van Hinsbergh VW, Engelse MA, Quax PH. Pericellular proteases in angiogenesis and vasculogenesis. Arterioscler Thromb Vasc Biol 2006;26:716–728. [PubMed: 16469948]
19. Egeblad M, Werb Z. New functions for the matrix metalloproteinases in cancer progression. Nat Rev Cancer 2002;2:161–174. [PubMed: 11990853]
20. Chun TH, Sabeh F, Ota I, Murphy H, McDonagh KT, Holmbeck K, Birkedal-Hansen H, Allen ED, Weiss SJ. MT1-MMP-dependent neovessel formation within the confines of the three-dimensional extracellular matrix. J Cell Biol 2004;167:757–767. [PubMed: 15545316]
21. Collen A, Hanemaaijer R, Lupu F, Quax PH, van Lent N, Grimbergen J, Peters E, Koolwijk P, van Hinsbergh VW. Membrane-type matrix metalloproteinase-mediated angiogenesis in a fibrin-collagen matrix. Blood 2003;101:1810–1817. [PubMed: 12393408]

22. Kroon ME, Koolwijk P, van Goor H, Weidle UH, Collen A, van der Pluijm G, van Hinsbergh VW. Role and localization of urokinase receptor in the formation of new microvascular structures in fibrin matrices. Am J Pathol 1999;154:1731–1742. [PubMed: 10362798]
23. Hiraoka N, Allen E, Apel IJ, Gyetko MR, Weiss SJ. Matrix metalloproteinases regulate neovascularization by acting as pericellular fibrinolysins. Cell 1998;95:365–377. [PubMed: 9814707]
24. Nakatsu MN, Sainson RC, Aoto JN, Taylor KL, Aitkenhead M, Perez-del-Pulgar S, Carpenter PM, Hughes CC. Angiogenic sprouting and capillary lumen formation modeled by human umbilical vein endothelial cells (HUVEC) in fibrin gels: the role of fibroblasts and Angiopoietin-1. Microvasc Res 2003;66:102–112. [PubMed: 12935768]
25. Chen X, Aledia AS, Ghajar CM, Griffith CK, Putnam AJ, Hughes CC, George SC. Prevascularization of a Fibrin-Based Tissue Construct Accelerates the Formation of Functional Anastomosis with Host Vasculature. Tissue Eng Part A. 2008
26. Weisel JW. Biophysics. Enigmas of blood clot elasticity. Science 2008;320:456–457. [PubMed: 18436761]
27. Xin X, Yang S, Ingle G, Zlot C, Rangell L, Kowalski J, Schwall R, Ferrara N, Gerritsen ME. Hepatocyte growth factor enhances vascular endothelial growth factor-induced angiogenesis in vitro and in vivo. Am J Pathol 2001;158:1111–1120. [PubMed: 11238059]
28. Armulik A, Abramsson A, Betsholtz C. Endothelial/pericyte interactions. Circ Res 2005;97:512–523. [PubMed: 16166562]
29. Brooks PC, Stromblad S, Sanders LC, von Schalscha TL, Aimes RT, Stetler-Stevenson WG, Quigley JP, Cheresh DA. Localization of matrix metalloproteinase MMP-2 to the surface of invasive cells by interaction with integrin alpha v beta 3. Cell 1996;85:683–693. [PubMed: 8646777]
30. Yana I, Sagara H, Takaki S, Takatsu K, Nakamura K, Nakao K, Katsuki M, Taniguchi S, Aoki T, Sato H, Weiss SJ, Seiki M. Crosstalk between neovessels and mural cells directs the site-specific expression of MT1-MMP to endothelial tip cells. J Cell Sci 2007;120:1607–1614. [PubMed: 17405818]
31. Cavallo-Medved D, Rudy D, Blum G, Bogyo M, Caglic D, Sloane BF. Live-cell imaging demonstrates extracellular matrix degradation in association with active cathepsin B in caveolae of endothelial cells during tube formation. Exp Cell Res 2009;315:1234–1246. [PubMed: 19331819]
32. Kniazeva E, Putnam AJ. Endothelial cell traction and ECM density influence both capillary morphogenesis and maintenance in 3-D. Am J Physiol Cell Physiol 2009;297:C179–C187. [PubMed: 19439531]
33. Grobelny D, Poncz L, Galardy RE. Inhibition of human skin fibroblast collagenase, thermolysin, and Pseudomonas aeruginosa elastase by peptide hydroxamic acids. Biochemistry 1992;31:7152–7154. [PubMed: 1322694]
34. Uttamchandani M, Wang J, Li J, Hu M, Sun H, Chen KY, Liu K, Yao SQ. Inhibitor fingerprinting of matrix metalloproteases using a combinatorial peptide hydroxamate library. J Am Chem Soc 2007;129:7848–7858. [PubMed: 17539636]
35. Wolf K, Mazo I, Leung H, Engelke K, von Andrian UH, Deryugina EI, Strongin AY, Brocker EB, Friedl P. Compensation mechanism in tumor cell migration: mesenchy-malamoeboid transition after blocking of pericellular proteolysis. J Cell Biol 2003;160:267–277. [PubMed: 12527751]
36. Grassl ED, Oegema TR, Tranquillo RT. Fibrin as an alternative biopolymer to type-I collagen for the fabrication of a media equivalent. J Biomed Mater Res 2002;60:607–612. [PubMed: 11948519]
37. Sternlicht MD, Werb Z. How matrix metalloproteinases regulate cell behavior. Annu Rev Cell Dev Biol 2001;17:463–516. [PubMed: 11687497]
38. Noda K, Ishida S, Shinoda H, Koto T, Aoki T, Tsubota K, Oguchi Y, Okada Y, Ikeda E. Hypoxia induces the expression of membrane-type 1 matrix metalloproteinase in retinal glial cells. Invest Ophthalmol Vis Sci 2005;46:3817–3824. [PubMed: 16186369]
39. Hamasuna R, Kataoka H, Moriyama T, Itoh H, Seiki M, Koono M. Regulation of matrix metalloproteinase-2 (MMP-2) by hepatocyte growth factor/scatter factor (HGF/SF) in human glioma cells: HGF/SF enhances MMP-2 expression and activation accompanying up-regulation of membrane type-1 MMP. Int J Cancer 1999;82:274–281. [PubMed: 10389763]

40. Jedeszko C, Victor BC, Podgorski I, Sloane BF. Fibroblast hepatocyte growth factor promotes invasion of human mammary ductal carcinoma in situ. Cancer Res 2009;69:9148–9155. [PubMed: 19920187]
41. Kroon ME, Koolwijk P, van der Vecht B, van Hinsbergh VW. Urokinase receptor expression on human microvascular endothelial cells is increased by hypoxia: implications for capillary-like tube formation in a fibrin matrix. Blood 2000;96:2775–2783. [PubMed: 11023511]
42. Caiolfa VR, Zamai M, Malengo G, Andolfo A, Madsen CD, Sutin J, Digman MA, Gratton E, Blasi F, Sidenius N. Monomer dimer dynamics and distribution of GPI-anchored uPAR are determined by cell surface protein assemblies. J Cell Biol 2007;179:1067–1082. [PubMed: 18056417]
43. Fata JE, Werb Z, Bissell MJ. Regulation of mammary gland branching morphogenesis by the extracellular matrix and its remodeling enzymes. Breast Cancer Res 2004;6:1–11. [PubMed: 14680479]
44. Freitas VM, Scheremeta B, Hoffman MP, Jaeger RG. Laminin-1 and SIKVAV a laminin-1-derived peptide, regulate the morphology and protease activity of a human salivary gland adenoid cystic carcinoma cell line. Oral Oncol 2004;40:483–489. [PubMed: 15006619]
45. Saunders WB, Bohnsack BL, Faske JB, Anthis NJ, Bayless KJ, Hirschi KK, Davis GE. Coregulation of vascular tube stabilization by endothelial cell TIMP-2 and pericyte TIMP-3. J Cell Biol 2006;175:179–191. [PubMed: 17030988]
46. Stratman AN, Saunders WB, Sacharidou A, Koh W, Fisher KE, Zawieja DC, Davis MJ, Davis GE. Endothelial cell lumen and vascular guidance tunnel formation requires MT1-MMP-dependent proteolysis in 3-dimensional collagen matrices. Blood 2009;114:237–247. [PubMed: 19339693]
47. Koolwijk P, Sidenius N, Peters E, Sier CF, Hanemaaijer R, Blasi F, van Hinsbergh VW. Proteolysis of the urokinase-type plasminogen activator receptor by metalloproteinase-12: implication for angiogenesis in fibrin matrices. Blood 2001;97:3123–3131. [PubMed: 11342439]
48. Lafleur MA, Handsley MM, Knauper V, Murphy G, Edwards DR. Endothelial tubulogenesis within fibrin gels specifically requires the activity of membrane-type-matrix metalloproteinases (MT-MMPs). J Cell Sci 2002;115:3427–3438. [PubMed: 12154073]
49. Hotary KB, Yana I, Sabeh F, Li XY, Holmbeck K, Birkedal-Hansen H, Allen ED, Hiraoka N, Weiss SJ. Matrix metalloproteinases (MMPs) regulate fibrin-invasive activity via MT1-MMP-dependent and -independent processes. J Exp Med 2002;195:295–308. [PubMed: 11828004]
50. Crisan M, Yap S, Casteilla L, Chen CW, Corselli M, Park TS, Andriolo G, Sun B, Zheng B, Zhang L, Norotte C, Teng PN, Traas J, Schugar R, Deasy BM, Badylak S, Buhring HJ, Giacobino JP, Lazzari L, Huard J, Peault B. A perivascular origin for mesenchymal stem cells in multiple human organs. Cell Stem Cell 2008;3:301–313. [PubMed: 18786417]
51. Hall B, Andreeff M, Marini F. The participation of mesenchymal stem cells in tumor stroma formation and their application as targeted-gene delivery vehicles. Handb Exp Pharmacol 2007:263–283. [PubMed: 17554513]
52. Dennis JE, Caplan AI. Analysis of the developmental potential of conditionally immortal marrow-derived mesenchymal progenitor cells isolated from the H-2Kb-tsA58 transgenic mouse. Connect Tissue Res 1996;35:93–99. [PubMed: 9084647]
53. Caplan AI. All MSCs are pericytes? Cell Stem Cell 2008;3:229–230. [PubMed: 18786406]
54. Song S, Ewald AJ, Stallcup W, Werb Z, Bergers G. PDGFRbeta+ perivascular progenitor cells in tumours regulate pericyte differentiation and vascular survival. Nat Cell Biol 2005;7:870–879. [PubMed: 16113679]
55. Baluk P, Hashizume H, McDonald DM. Cellular abnormalities of blood vessels as targets in cancer. Curr Opin Genet Dev 2005;15:102–111. [PubMed: 15661540]
56. Tomasek JJ, Gabbiani G, Hinz B, Chaponnier C, Brown RA. Myofibroblasts and mechano-regulation of connective tissue remodelling. Nat Rev Mol Cell Biol 2002;3:349–363. [PubMed: 11988769]
57. Kalluri R, Zeisberg M. Fibroblasts in cancer. Nat Rev Cancer 2006;6:392–401. [PubMed: 16572188]
58. Overall CM, Kleifeld O. Towards third generation matrix metalloproteinase inhibitors for cancer therapy. Br J Cancer 2006;94:941–946. [PubMed: 16538215]

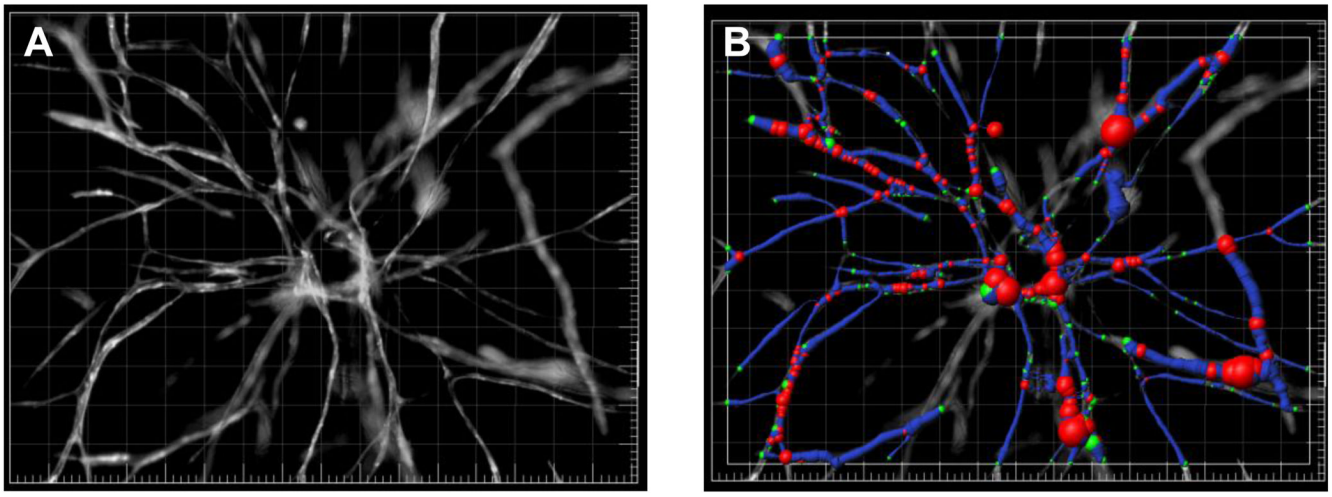

Figure 1. Depiction of network visualization and tracing

A) Low magnification fluorescent images of day 7 capillary networks were segmented based on a constant threshold of a background corrected image. Minimum and maximum thresholds were set to delineate capillaries from noise or beads/nodes, respectively, before applying the Angiogenesis Tube Formation Application Module in Metamorph imaging software. B) A sample tracing generated by automated processing. The filament tracing function was used to visualize networks (blue) using Imaris.

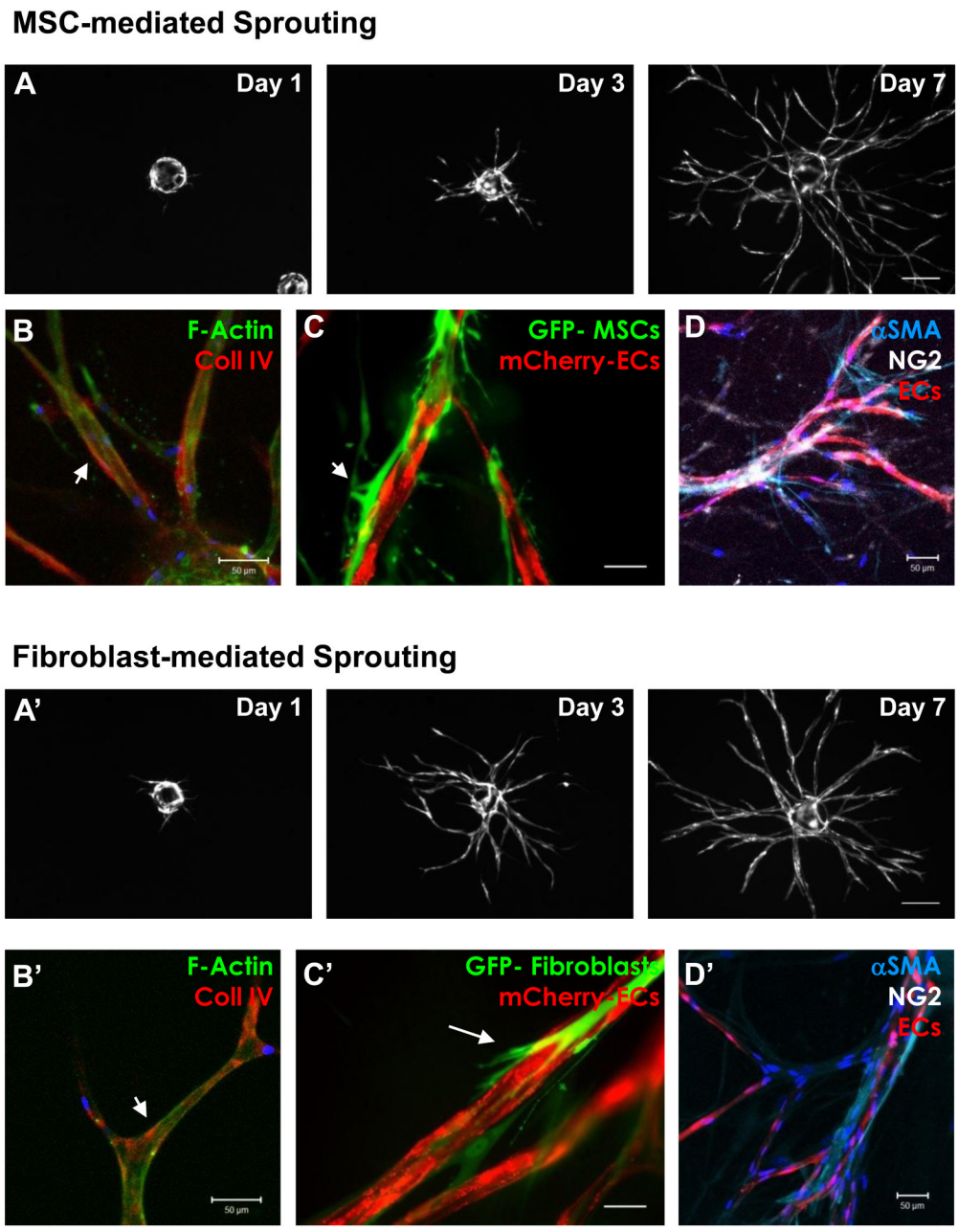

Figure 2. MSCs and fibroblasts stimulate ECs to form mature capillary networks

MSCs (A–D) or fibroblasts (A'–D') were interspersed throughout fibrin ECMs in the presence of microcarrier beads coated with mCherry-transduced ECs. A, A') Beads were monitored over a 7 day period and imaged at days 1, 3, and 7. Red channel fluorescence (i.e., ECs) is shown. Scale = 200 μm. B, B') Cultures were fixed and IF stained at day 7 for F-actin (green) and collagen IV (red). Basement membrane deposition (white arrows) was observed in both conditions. Scale = 50 μm. C, C') Mesenchymal cells expressing GFP were interspersed with mCherry-transduced EC. Physical association of both cell types was observed in both conditions (white arrows). Scale = 25 μm. D, D') Cultures containing mCherry-transduced ECs and either MSCs (D) or fibroblasts (D') were fixed and IF stained for pericyte markers

αSMA (aqua) and NG2 (white). DAPI-stained nuclei are visible in the blue channel. Scale = 50μm.

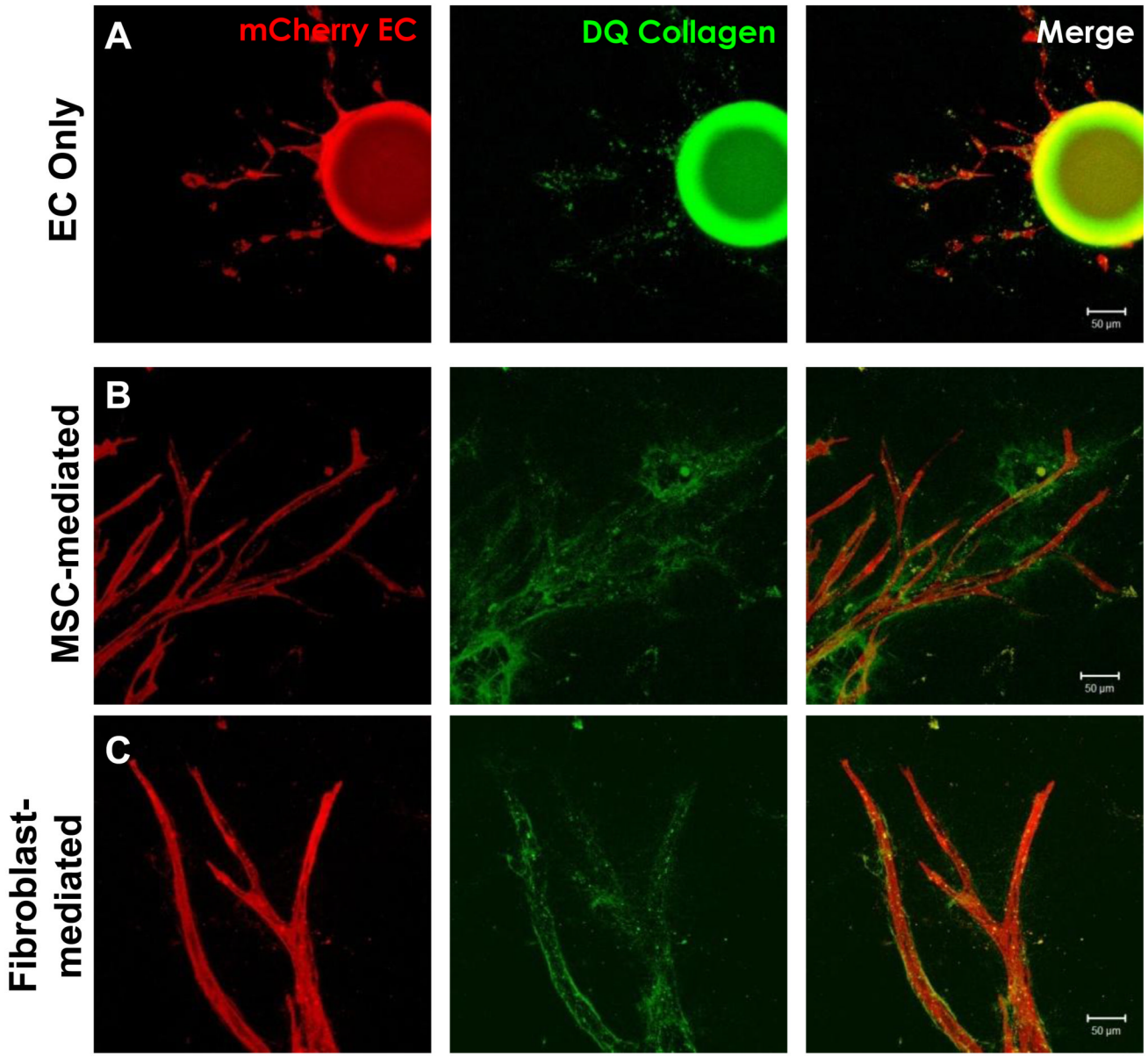

Figure 3. Interstitial cell-mediated capillary morphogenesis is accompanied by periendothelial proteolysis

mCherry-transduced ECs were cultured within fibrin ECMs containing 1% DQ Collagen either A) alone, B) with MSCs, or C) with fibroblasts. Red (mCherry-ECs), green (proteolyzed ECM), and merged channels are shown. Autofluorescence from the microcarrier bead is evident in A). Scales = 50 μm.

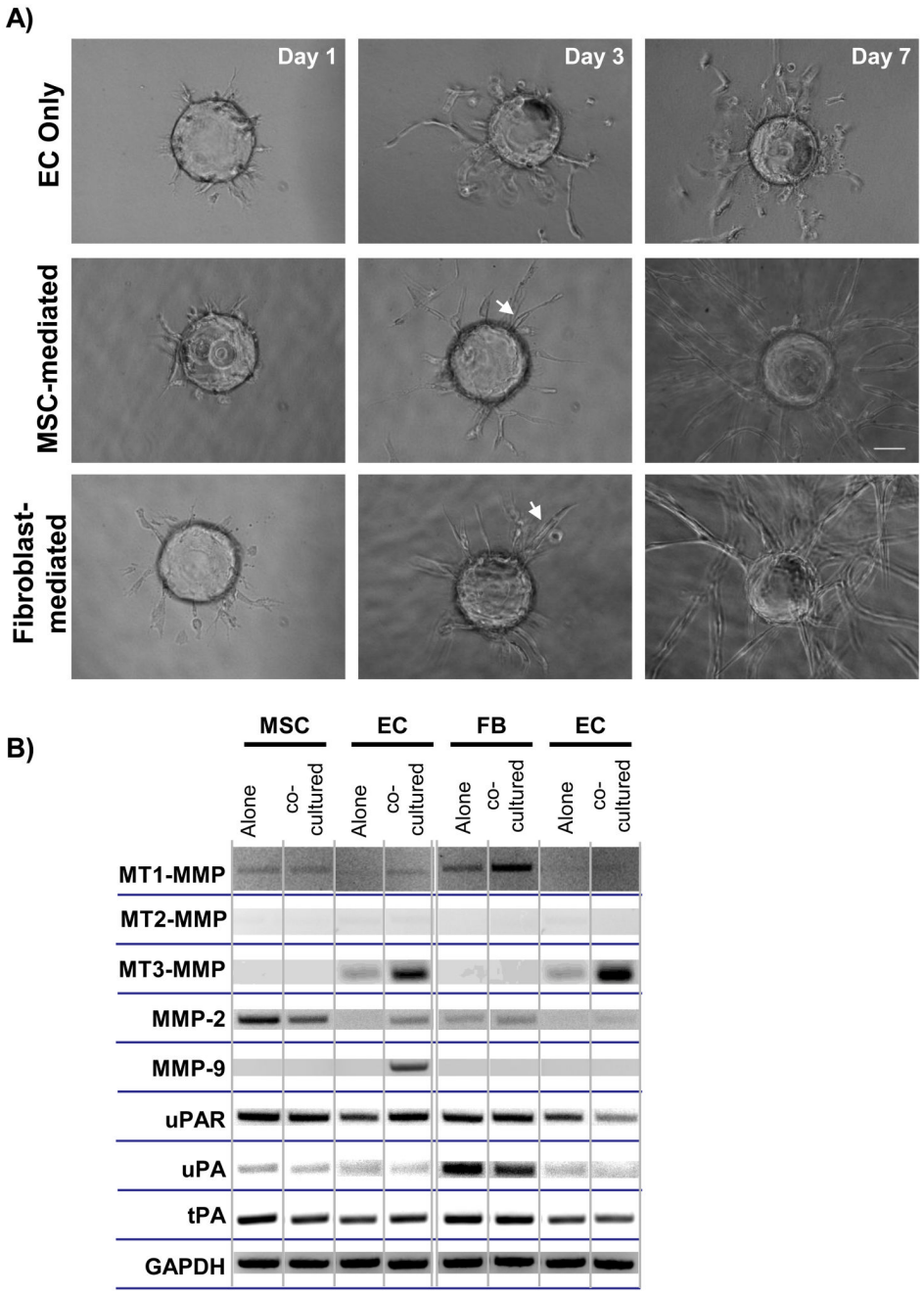

Figure 4. Onset of capillary morphogenesis coincides with upregulated expression of fibrinolytic enzyme transcripts by EC

A) Brightfield images (10x) of EC-coated microcarrier beads at days 1, 3, and 7 cultured either alone (top row), with overlaid MSCs (middle row), or with overlaid fibroblasts (bottom row). Lumen formation is first evident in both co-cultures by day 3 (white arrows). Scale = 100 μm. B) Fibrinolytic enzyme and GAPDH (internal control) transcript expression for mesenchymal cells and ECs cultured separately ("alone") or together ("co-cultured") probed via RT-PCR (day 3). This experiment was repeated twice and a representative sample is shown.

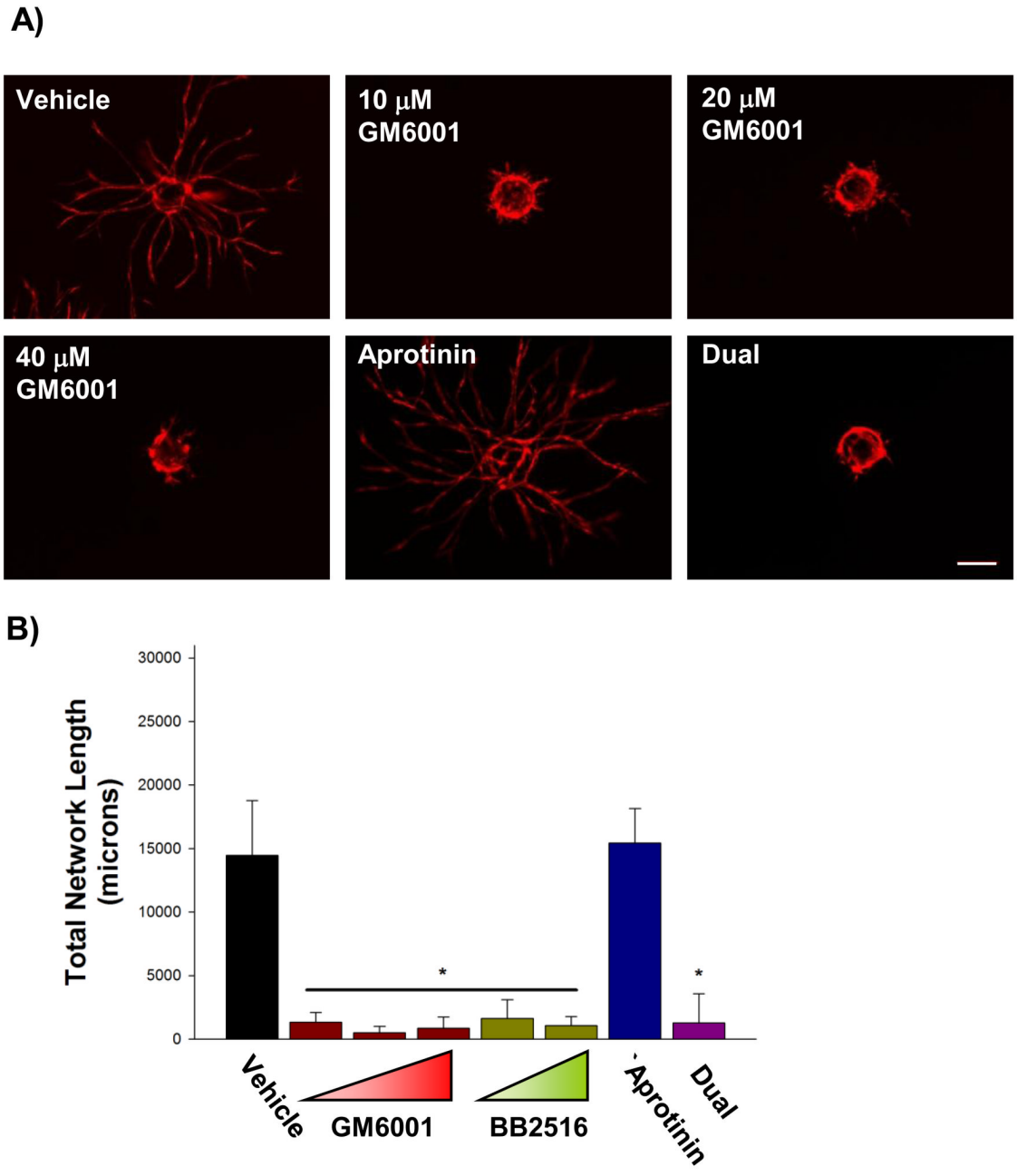

Figure 5. Broad spectrum inhibition reveals that MSC-mediated capillary morphogenesis is MMP dependent

A) mCherry-transduced ECs were coated onto microcarrier beads and cultured within fibrin matrices interspersed with unlabelled MSCs. Shown are fluorescent images at day 7 of capillary network formation in vehicle (DMSO) treated cultures, those treated with 10 μM, 20 μM, or 40 μM of the broad spectrum MMP inhibitor GM6001, with 2.2 μM of the serine protease inhibitor aprotinin, or with a combination of GM6001 (10 μM) and aprotinin (2.2 μM) ("both"). Scale = 200 μm. B) Total network lengths were quantified from a minimum of 10 images over 2–3 independent experiments per condition as described in *Materials and Methods*. Applied concentrations of BB2516 were 3.3 and 10 μM. * $P<0.05$ when comparing the indicated

conditions to vehicle control. One-way ANOVA followed by post-test analysis using Dunn's method was used to compare treatment groups.

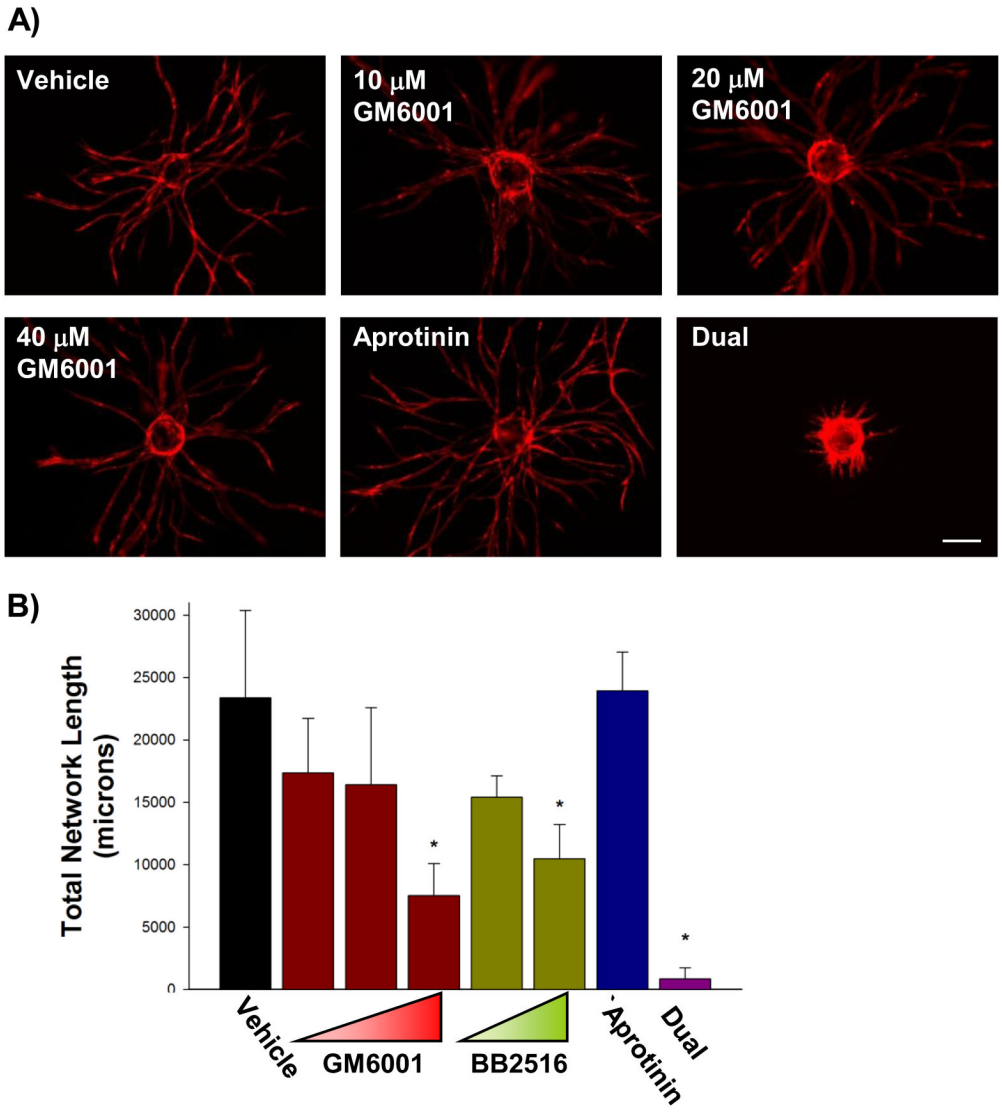

Figure 6. Broad spectrum inhibition reveals that fibroblast-mediated capillary morphogenesis is both MMP and serine protease dependent

A) mCherry-transduced ECs were coated onto microcarrier beads and cultured within fibrin matrices interspersed with unlabelled fibroblasts. Shown are fluorescent images at day 7 of capillary network formation in vehicle (DMSO) treated cultures, those treated with 10 μM, 20 μM, or 40 μM of the broad spectrum MMP inhibitor GM6001, with 2.2 μM of the serine protease inhibitor aprotinin, or with a combination of GM6001 (10 μM) and aprotinin (2.2 μM) ("both"). Scale = 200 μm. B) Total network lengths were quantified from a minimum of 10 images over 2–3 independent experiments per condition as described in *Materials and Methods*. Applied concentrations of BB2516 were 3.3 and 10 μM. * $P<0.05$ when comparing the indicated conditions to vehicle control. One-way ANOVA followed by post-test analysis using Dunn's method was used to compare treatment groups.

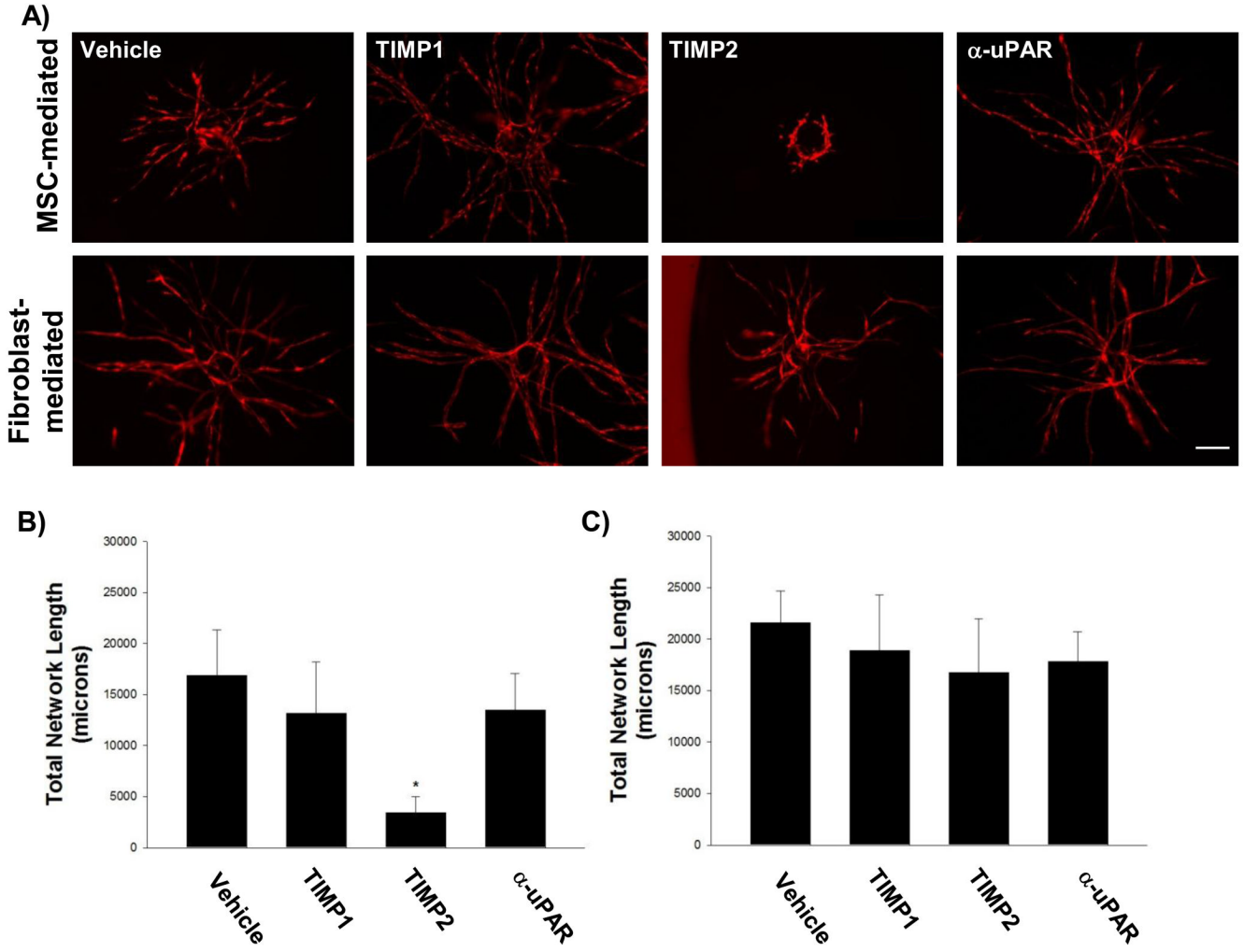

Figure 7. Endogenous inhibitors confirm that mesenchymal cells stimulate capillary morphogenesis via distinct proteolytic mechanisms

A) mCherry-transduced ECs were coated onto microcarrier beads and cultured within fibrin matrices interspersed with unlabelled MSCs (top row) or fibroblasts (bottom row). Shown are fluorescent images at day 7 of capillary network formation in vehicle (PBS) treated cultures, or those treated with 5 μg/mL TIMP1 or TIMP2, or with 25 μg/mL of a function blocking antibody directed towards uPAR (α-uPAR). Scale = 200 μm. B, C) Total network lengths were quantified from a minimum of 5 images over 2–3 independent experiments per condition as described in *Materials and Methods* for EC-MSC (B) and EC-fibroblast (C) cultures. * $P < 0.001$ when compared to vehicle control. One-way ANOVA followed by post-test analysis using the Holm-Sidak method was used to compare treatment groups.

Table I

Description of primers used for RT-PCR

Gene	Primers (F = forward; R = reverse)	Anneal Temp. (°C)	Amplicon size (bp)
MT1-MMP	F: 5'-GCTTGCAAGTAACAGGCAAA-3' R: 5'-AAATTCTCCGTGTCCATCCA-3'	57	589
MT2-MMP	F: 5'-TCGACGAAGAGACCAAGGAGT-3' R: 5'-CTTGAAGTTGTCAACGTCCT-3'	55	578
MT3-MMP	F: 5'-ATGTGCTACAGTCTGCGGAAC-3' R: 5'-TATCCACATCACGTTTGCCA-3'	59	461
MMP2	F: 5'-CAAGTGGTCCGTGTGAAGTA-3' R: 5'-CTTGCGGTCATCATCGTAGT-3'	56	504
MMP9	F: 5'-GACCTCAAGTGGCACCACCA-3' R: 5'-GTGGTACTGCACCAGGGCAA-3'	62	483
uPAR	F: 5'-ACAGGAGCTGCCCTCGCGAC-3' R: 5'-GAGGGGGATTTCAGGTTTAGG -3'	58	414
uPA	F: 5'-GGCAGCAATGAACTTCATCAAGTTCC-3' R: 5'-TATTTCACAGTGCTGCCCTCCG-3'	56	135
tPA	F: 5'-CCAGCAACATCAGTCATGGC-3' R: 5'-GCACTTCCCAGCAAATCCTTC-3'	60	205
GAPDH	F: 5'-CCCTGTTGCTGTAGCCGTA-3' R: 5'-CCGGTGCTGAGTATGTCG-3'	58	442